CHEMISTRY
A EUROPEAN JOURNAL

DOI: 10.1002/chem.200501017

Mechanism and *exo*-Regioselectivity of Organolanthanide-Mediated Intramolecular Hydroamination/Cyclization of 1,3-Disubstituted Aminoallenes: A Computational Study

Sven Tobisch*[a]

Abstract: The complete catalytic reaction course for the organolanthanide-assisted intramolecular hydroamination/cyclization (IHC) of 4,5-heptadien-1-ylamine by a prototypical [$(\eta^5\text{-}Me_5C_5)_2LuCH(SiMe_3)_2$] precatalyst has been critically scrutinized by employing a reliable DFT method. A computationally verified mechanistic scenario for the IHC of 1,3-disubstituted aminoallene substrates has been proposed that is consistent with the empirical rate law determined by experiment and accounts for crucial experimental observations. It involves kinetically rapid substrate association and dissociation equilibria, facile and reversible intramolecular allenic C=C insertion into the Ln–N bond, and turnover-limiting protonation of the azacycle's tether functionality, with the amine-amidoallene–Ln adduct complex representing the catalyst's resting state. This mechanistic scenario bears resemblance to the mechanism that has been recently proposed in a computational exploration of aminodiene IHC. The unique features of the IHC of the two substrate classes are discussed. Furthermore, the thermodynamic and kinetic factors that control the regio- and stereoselectivity of aminoallene IHC have been elucidated. These achievements have provided a deeper insight into the catalytic structure–reactivity relationships in organolanthanide-assisted cyclohydroamination of unsaturated C–C functionalities.

Keywords: density functional calculations · homogeneous catalysis · hydroamination · lanthanides · reaction mechanisms

Introduction

Catalytic hydroamination, that is, the addition of amine R_2N–H bonds across unsaturated carbon–carbon functionalities, is a highly valuable, desirable, and atom-economical means of synthesizing organonitrogen compounds that have a diverse range of applications in organic chemistry.[1] Organolanthanides[2] are established as highly efficient catalysts for both intermolecular hydroamination and intramolecular hydroamination/cyclization (IHC) reactions that are characterized by high turnover frequencies and versatile reaction scope.[3,4] The cyclohydroamination reaction mediated by organolanthanide compounds is of fundamental importance in synthetic organic chemistry because it provides a concise route to the generation of functionalized azacycles with high regio- and stereoselectivity. Several research groups have contributed to the development of the IHC of a variety of amine-tethered carbon–carbon unsaturated compounds,[3,4] namely, aminoalkenes,[5,6] aminoalkynes,[7,8] aminoallenes,[9] and aminodienes.[10] Of the various C–C unsaturated compounds, aminoallenes have received particular interest as attractive substrates for the construction of naturally occurring alkaloid skeletons.[9b] The intramolecular cyclohydroamination of aminoallenes by early[11] and late[12] transition-metal complexes has been advanced by several groups.

On the basis of comprehensive kinetic and mechanistic investigations, Marks proposed a generally accepted mechanistic scenario for organolanthanide-catalyzed IHC that is characterized by the following features common to the various unsaturated C–C functionalities:[3] 1) smooth precatalyst activation through protonolysis by the substrate, 2) a large negative activation entropy $\Delta S^{\neq}$, and 3) a reaction rate that is first order in [catalyst] and zeroth order in [amine substrate]. These observations indicate an identical turnover-limiting step for the IHC of the various substrates, which Marks suggested to generally be the intramolecular C–C

[a] Priv.-Doz. Dr. S. Tobisch
Institut für Anorganische Chemie
der Martin-Luther-Universität Halle-Wittenberg
Fachbereich Chemie, Kurt-Mothes-Strasse 2, 06210 Halle (Germany)
E-mail: tobisch@chemie.uni-halle.de

Supporting information for this article is available on the WWW under http://www.chemeurj.org/ or from the author.

multiple-bond insertion into the Ln–N bond which has a highly organized, compact transition-state (TS) structure.[3]

Two computational studies of the mechanism of the organolanthanide-mediated cyclohydroamination of aminoalkenes[13] and conjugated aminodienes[14a] have recently been reported. Consistent with the general mechanistic proposal, the cyclization is predicted to be rate-controlling for aminoalkenes.[13] Protonolysis of the alkyl–Ln functionality of the azacyclic intermediate, however, has been computed to be only slightly disfavored kinetically ($\Delta\Delta G^{\neq} = 1.2$ kcal mol^{-1}) compared with intramolecular C–N bond formation. The origin of the measured large negative $\Delta S^{\neq}_{tot}$, however, is not understood thus far for the IHC of aminoalkenes.[13] On the other hand, a revised mechanistic scenario has been proposed for conjugated aminodiene substrates that is consistent with experimental observations.[14a] It involves kinetically mobile substrate association/dissociation equilibria, facile and reversible intermolecular diene insertion into the Ln–N bond, and turnover-limiting protonolysis of the η^3-butenyl–Ln functionality with the amine-amidodiene–Ln adduct complex representing the catalyst's resting state.[14a]

This apparent difference in the working mechanism for the IHC of the two substrate classes prompted us to investigate in detail the salient mechanistic features of the organolanthanide-mediated cyclohydroamination of 1,3-disubstituted aminoallenes, which has been thoroughly studied experimentally.[9] The aim of this study was twofold: first, to elucidate computationally whether the general mechanism proposed by Marks is operative or has to be modified for aminoallene substrates, and second, to unravel the key catalytic question about what the kinetic and thermodynamic factors are that control the selectivity (see below). Herein we present, to the best of our knowledge, the first comprehensive computational mechanistic investigation of the organolanthanide-supported IHC of 1,3-disubstituted aminoallenes that covers the complete sequence of crucial elementary steps. This study represents an extension of our systematic computational exploration of the catalytic structure–reactivity relationships in the IHC of various unsaturated C–C functionalities.

Computational Model and Methods

Model: In this DFT investigation, we report the exploration of the cyclohydroamination of 4,5-heptadien-1-ylamine (**1**), as a prototypical 1,3-disubstituted aminoallene substrate, in the presence of the [(η^5-Me_5C_5)$_2$LuCH($SiMe_3$)$_2$] precatalyst (**2**), for which a detailed kinetic study has been reported.[9c] The computational studies include the scrutinization of alternative pathways for each of the crucial elementary steps of the tentative catalytic cycle displayed in Scheme 1.

Methods: All DFT calculations were performed with the TURBOMOLE program package[16] using the BP86 density functional,[17] which has already been applied successfully to the description of the energetic and structural aspects of organolanthanide compounds.[18] The suitability of the BP86 functional for the reliable determination of the energy profile for the organolanthanide-mediated cyclohydroamination of conjugated aminodienes[14a] and the ring-opening polymerization of methylenecycloalkanes[19] has been demonstrated. Further details, together with a description of the computational methodology employed, are given in the Supporting Information. All the drawings were prepared by using the StrukEd program.[20]

Results and Discussion

This report of the computational exploration of aminoallene IHC is divided into four parts. In the first section the proposed catalytic reaction course is discussed. The second part reports on the detailed step-by-step exploration of the elementary steps outlined in Scheme 1. The discussion is focused on the most favorable of the several possible pathways for a given step in the catalytic course, while alternative, but less likely, pathways are tackled only briefly. The results are compared with those reported in the recent computational study of aminodiene cyclohydroamination.[14a,21] The condensed free-energy profile is presented in the third part. Whether the general mechanism proposed by Marks[3] is consistent with the predicted ΔG profile is discussed. A further section is devoted to the control of regio- and stereoselectivity.

Proposed catalytic reaction course: Organolanthanide complexes of the general type [Cp*$_2$LnCH(TMS)$_2$] (Cp* = η^5-Me_5C_5; Ln = La, Sm, Y, Lu; TMS = $SiMe_3$) have been reported to serve as effective precatalysts for the IHC of aminoallenes to afford functionalized five- and six-membered azacycles.[9] This transformation can be managed so as to proceed with almost complete regioselectivity and high diastereoselectivity.[3,9] Scheme 1 shows a general catalytic cycle for the organolanthanide-mediated cyclohydroamination of aminoallene substrate **1** by the [Cp*$_2$LnCH(TMS)$_2$] starting material **2**. Precatalyst **2** is activated through protonolysis by substrate **1** to liberate the $CH_2(TMS)_2$ hydrocarbon ligand and generate the catalytically active amidoallene–Ln compound **3**. The allenic C=C linkage subsequently adds across the Ln–N functionality of complex **3** to afford azacyclic intermediates. This process can occur through regioisomeric 5-*exo* and 6-*endo* cyclization to give rise to five- and six-membered azacyclic intermediates **4** and **5**, respectively, that bear a functionalized tether. In the 6-*endo* cyclization product the azacycle moiety can be coordinated through its nitrogen-donor functionality to the lanthanide center, **5**, or alternatively through an allylic interaction, **5′**.[15] These two modes are likely to be easily interconvertible. The ensuing protonolysis of the azacyclic insertion products **4** and **5** by substrate **1** yields first cycloamine-amido–Ln compounds **6–8** from which **3** is regenerated by the ready liberation of cycloamine products **P6–P8**, thereby completing the catalytic cycle. Protonation of the C^6 carbon atom in **4** affords the 2-(prop-1-enyl)pyrrolidines **P6*E*** and **P6*Z*** with a side-chain of *E* and *Z* configuration, respectively. For the protonolysis of **5** and **5′** to follow the regioisomeric paths for proton transfer onto the C^7 and C^5 centers, 6-ethyl-1,2,3,4-tetrahydropyridine (**P7**) and 2-ethylidenepiperidine (**P8**) are initially generated, respectively, both of which are readily transformed

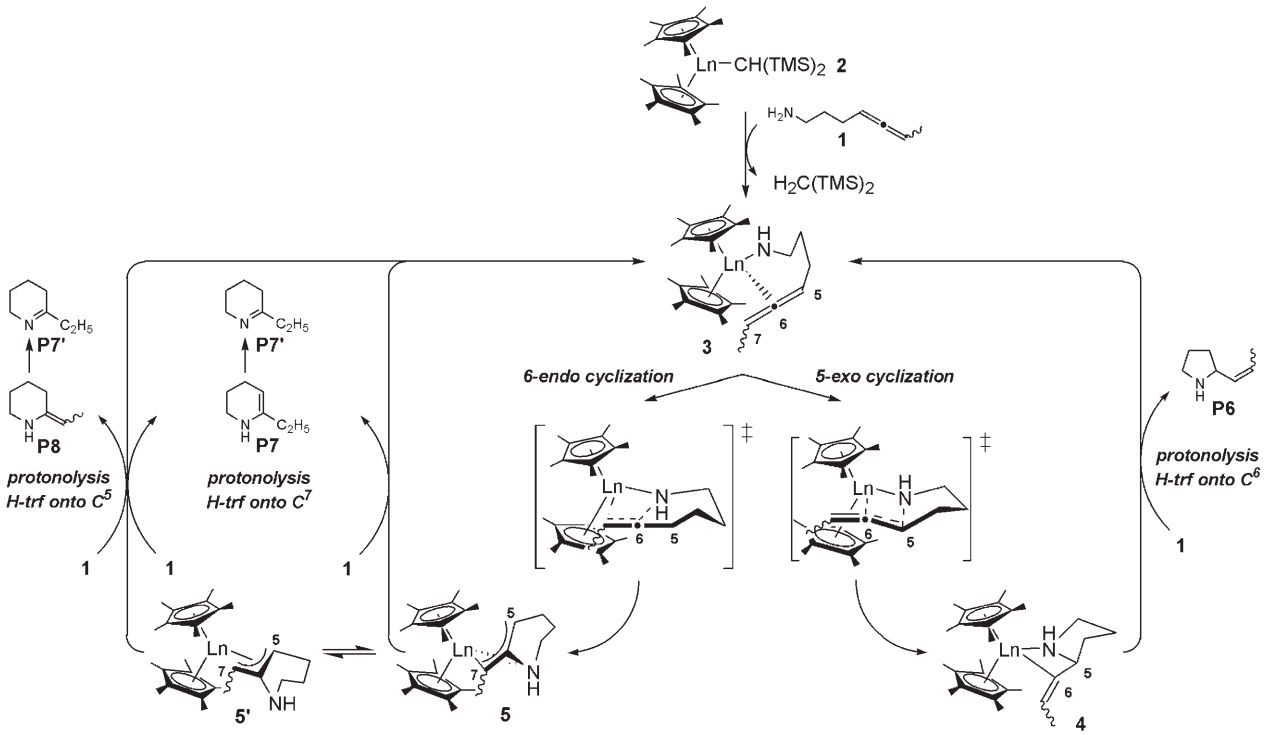

Scheme 1. General catalytic reaction course for the organolanthanide-mediated intramolecular hydroamination/cyclization of aminoallenes to afford functionalized five- and six-membered azacycles based on the experimental studies of Marks and co-workers.[3,9] The 4,5-heptadien-1-ylamine (**1**) and the [Cp*$_2$LnCH(TMS)$_2$] complex (**2**) were chosen as the prototypical 1,3-disubstituted aminoallene substrate and precatalyst, respectively. The cycloamine-amido−Ln compounds **6**–**8** have been omitted for the sake of clarity.

into the thermodynamically favorable 2-ethyl-3,4,5,6-tetrahydropyridine (**P7′**) through a 1,3-hydrogen shift.

The cyclohydroamination of the 4,5-heptadien-1-ylamine substrate (**1**) with [Cp*$_2$LuCH(TMS)$_2$] is a rapid transformation.[9a,c] 2-Propenylpyrrolidines **P6*Z*** and **P6*E*** are exclusively generated in an 88:12 ratio with no evidence of the alternative six-membered azacycles.[9a,c,d] Hence, the IHC of the prototypical 1,3-disubstituted aminoallene **1** proceeds with complete regioselectivity and good *Z* double-bond selectivity. Experiments revealed an empirical rate law [Eq. (1)] that predicts first-order and zeroth-order behavior in [catalyst] and [aminoallene substrate], respectively, and showed that the process is associated with a negative activation entropy ($\Delta S^{\neq} = -16.48(4.3)$ cal mol^{-1} K^{-1}).[9c]

$$\text{velocity} = k[\text{substrate}]^0[\text{Ln}]^1 \quad (1)$$

Exploration of the crucial elementary steps

Precatalyst activation: For IHC to be initiated, precatalyst **2** has to be smoothly transformed into the amidoallene−Lu compound **3** through protonolysis by substrate **1** with liberation of the $CH_2(TMS)_2$ ligand. The structural features of this conversion have already been analyzed in detail in our previous study.[14a] Therefore, the focus here is on the energetics of the reaction (Table 1), while the key species are included in the Supporting Information (Figure S1).

Table 1. Enthalpies and free energies of activation and reaction for the protonolysis of precatalyst **2** by aminoallene substrate **1**.[a,b]

Protonolysis path	Substrate encounter complex	TS	Products[c]
1+**2**→ **3**+CH_2-(TMS)$_2$	−3.3/*6.1* (**2**-S)	10.0/*20.0* ($\Delta S^{\neq}$ = −33.5 eu)[d]	−29.2/*−30.1* (**3′**) −26.4/*−25.4* (**3s″**)

[a] The total activation barriers and reaction energies are given relative to {**1**+**2**}. [b] The enthalpies and free energies of activation ($\Delta H^{\neq}/\Delta G^{\neq}$) and reaction ($\Delta H/\Delta G$) are given in kilocalories per mole; the numbers in italic type are the Gibbs free-energies. [c] See the text (or Figure S1) for a description of the various isomers of **3**. [d] The activation entropy is given in entropic units ≡cal mol^{-1} K^{-1}.

The formation of the substrate encounter complex **2**-S is endergonic ($\Delta G = 6.1$ kcal mol^{-1} relative to {**1**+**2**})[22] as a result of the entropy penalty for bimolecular substrate association. The ensuing protonolysis of the Lu−C bond requires a free energy of activation of 20.0 kcal mol^{-1} to yield **3** in an exergonic process that is driven by a large thermodynamic force of −30.1 kcal mol^{-1} (Table 1). This confirms the observation by NMR spectroscopy that precatalyst conversion occurs in a clean and almost quantitative fashion.[9c] Activation of the [Cp*$_2$LaCH(TMS)$_2$] starting material in aminodiene IHC has a barrier of 14.3 kcal mol^{-1} ($\Delta G^{\neq}$).[14a] Inspection of the key species reveals that the kinetically more ex-

pensive protonolysis of the Lu–C bond in precatalyst **2** is related to the difference in the Ln^{3+} ionic radius ($Lu^{3+} < La^{3+}$)[23] such that greater reorganization is required for the lutetium-based system to form the TS structure.

The catalytically active compound **3** exists as readily interconvertible[22] isomers **3′** and **3″** that bear an η^1-amidoallene and a chair-like chelating amidoallene moiety, respectively (Figure S1), with species **3′** thermodynamically prevalent (Table 1). Compound **3** complexes substrate **1**, which is always present in excess,[9d] through a kinetically facile[22] association step.[24] Substrate uptake comes at the expense of the chelating amidoallene–Lu moiety (Figure S1)[25] such that **3′**-S with a noncoordinating amidoallene functionality becomes the prevalent adduct species. The enthalpic stabilization for **3′**+**1**→**3′**-S is large enough to compensate for the associated entropic costs (Table 2). Accordingly, complex **3** is predominantly present as the substrate adduct **3′**-S under the catalytic reaction conditions (cf. the Gibbs free-energy profile section).[9d]

Intramolecular cyclization: After the smooth transformation of the starting material **1** into the amidoallene–Lu compound **3**, the allenic C=C bond is inserted into the Lu–N functionality of this catalyst complex through either a 5-*exo* or 6-*endo* cyclization process (Scheme 1). The alternative paths are structurally characterized in Figure 1 (5-*exo*) and Figure S2 (6-*endo*), while the complete energetics of this step are collected in Table 2.

Species **3″** with a chelating amidoallene moiety is the direct precursor of the minimum energy path for C–N bond formation to afford **4** and **5**,**5′** (Figure 1 and Figure S2). Two pathways can be envisaged for each of the regioisomeric cyclization paths, which are distinguished by the orientation of the terminal C^8-methyl substituent relative to the C^5–C^6 (5-*exo*) and N–H (6-*endo*) bonds, respectively, as being *anti* or *syn* disposed (Scheme 2). Chair-like TS structures with an amidoallene moiety that is distorted to only a small extent relative to the precursor are encountered along the 5-*exo* path (Figure 1). Because the terminal C^8-methyl group is in a coplanar arrangement with respect to the emerging C^5–N bond, steric interactions with the catalyst backbone are likely to be less pronounced for the *syn* pathway (Scheme 2). On the other hand, the amidoallene moiety requires significant reorganization if it is to reach the TS along the 6-*endo* path, in which the C^8-methyl substituent adopts a position perpendicular to the emerging C^6–N bond (Figure S2). This causes substantial unfavorable steric interactions with the Cp* rings, which, however, owing to the symmetrical nature of the catalyst backbone, should be of similar magnitude in both the *anti* and *syn* pathways.

These structural features are paralleled in the computed free-energy profiles (Table 2). Intramolecular C–N bond formation is seen to be sensitive to steric factors. The formation of **4** proceeds preferentially through the *syn* pathway requiring a moderate activation energy ($\Delta G^{\neq}$ = 9.1 kcal mol^{-1}), while increased steric pressure along the *anti* pathway raises the barrier by 3.2 kcal mol^{-1} ($\Delta\Delta G^{\neq}$). Ring closure through the 6-*endo* path suffers as a result of severe repulsive interactions between the C^8-methyl and Cp* moieties, thereby rendering this path significantly more expensive kinetically. Note that this affects the *anti* and *syn* pathways ($\Delta G^{\neq}$ = 18.8–19.3 kcal mol^{-1}) to comparable extents. Steric factors not only control the kinetics, but can also influence the product stability. For the 5-*exo* cyclization process, steric effects discriminate kinetically between the *anti* and *syn* pathways, but not thermodynamically, as both pathways are driven by an exergonicity ($\Delta G = -4.3$ kcal mol^{-1}) of identical magnitude. On the other hand, the 6-*endo* ring closure is predicted to have comparable kinetics along the two pathways, while the orientation of the C-8-methyl substituent largely affects the stability of the insertion products. For **5** the *anti* isomer **5a** is favored, while the *syn*-η^3-allylic–Lu form **5s′** is prevalent for **5′**; in both cases the reason for these preferences can be traced back to steric factors (see Figure S2).

Intramolecular cyclization is predicted to be a kinetically

Table 2. Enthalpies and free energies of activation and reaction for the cyclization of **3** by alternative regioisomeric 5-*exo* and 6-*endo* paths.[a,b]

Cyclization path	Precursor[c]	TS	Product[d]
5-*exo*	0.0/*0.0* (**3′**)		
syn pathway	2.8/*4.8* (**3s″**)	5.8/*9.1* ($\Delta S^{\neq} = -11.0$ eu)[e]	−6.5/*−4.3* (**4s**)
anti pathway	7.2/*9.6* (**3a″**)	8.4/*12.3* ($\Delta S^{\neq} = -13.1$ eu)[e]	−6.9/*−4.3* (**4a**)
6-*endo*	0.0/*0.0* (**3′**)		
syn pathway		16.7/*19.3* ($\Delta S^{\neq} = -8.9$ eu)[e]	−6.5/*−3.5* (**5s**) −10.6/*−6.6* (**5s′**)
anti pathway		15.8/*18.8* ($\Delta S^{\neq} = -10.2$ eu)[e]	−12.3/*−8.5* (**5a**) −3.9/*−0.1* (**5a′**)
	aminoallene substrate-assisted process[f]		
5-*exo*	−12.4/*−2.9* (**3′**-S)		
syn pathway	−8.9/*0.2* (**3s″**-S)	17.0/*27.9* ($\Delta S^{\neq} = -36.3$ eu)[e]	−6.2/*4.3* (**4s**-S)
anti pathway	−8.8/*0.2* (**3a″**-S)	21.3/*32.2* ($\Delta S^{\neq} = -36.6$ eu)[e]	−5.8/*5.1* (**4a**-S)
6-*endo*	−12.4/*−2.9* (**3′**-S)		
syn pathway		22.3/*32.7* ($\Delta S^{\neq} = -34.7$ eu)[e]	−7.5/*4.2* (**5s**-S) −7.9/*4.6* (**5s′**-S)[g]
anti pathway		23.2/*32.8* ($\Delta S^{\neq} = -32.1$ eu)[e]	−10.9/*1.3* (**5a**-S) −7.2/*5.2* (**5a′**-S)[g]

[a] The total activation barriers, reaction energies, and activation entropies are given relative to the thermodynamically favored isomer of **3**, namely, **3′** with a nonchelating allene functionality. [b] The enthalpies and free energies of activation ($\Delta H^{\neq}/\Delta G^{\neq}$) and reaction ($\Delta H/\Delta G$) are given in kilocalories per mole; the numbers in italic type are the Gibbs free-energies. [c] See the text (or Figure S1) for a description of the various isomers of **3** and **3**-S. [d] See Scheme 1 for a description of the azacyclic cyclization products. [e] The activation entropy is given in entropic units, ≡cal mol^{-1} K^{-1}. [f] The process to be assisted by an additionally coordinating aminoallene molecule has been investigated with **1** as the substrate (Figure S3 and S4). The total activation barriers, reaction energies, and activation entropies are given relative to {**3′**+**1**}. [g] The modes favored for azacycle–Lu coordination are η^3-allylic (**5s′**-S) and η^1-allylic (**5a′**-S).

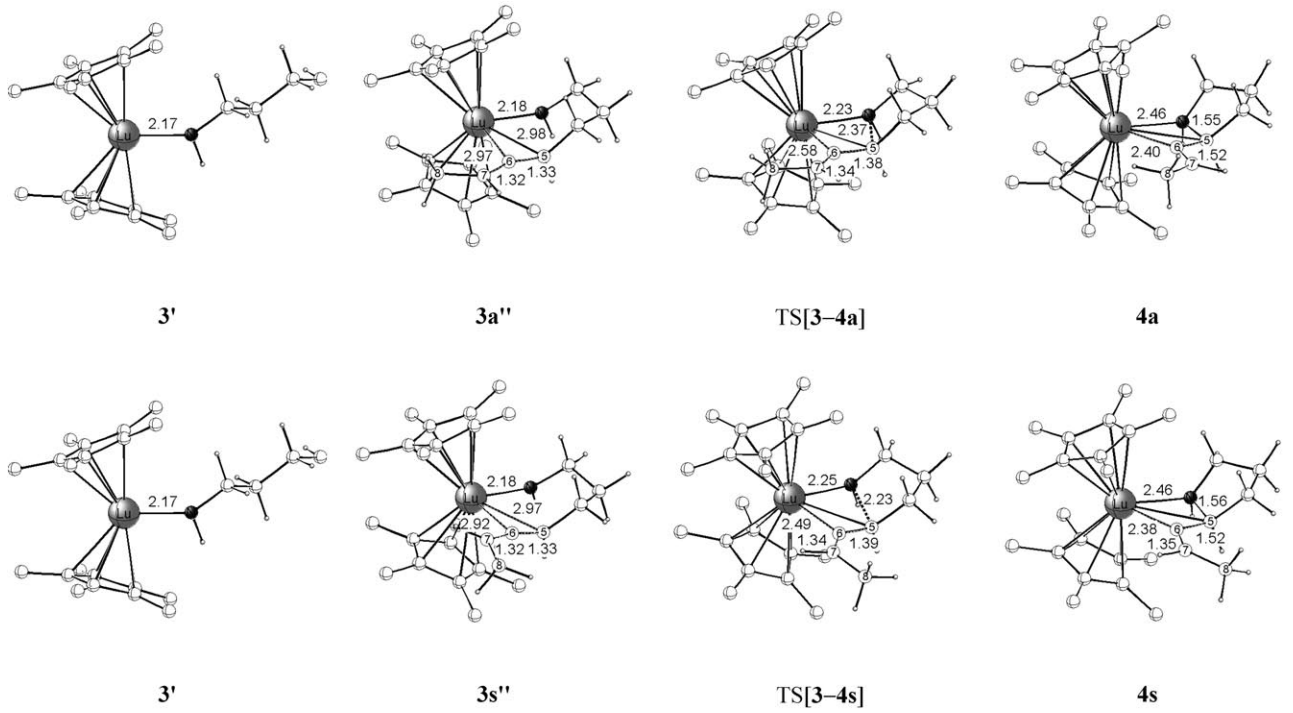

Figure 1. Selected structural parameters [Å] of the optimized structures of the key species for the *anti* (top) and *syn* (bottom) pathways of 5-*exo* cyclization. The cut-off for drawing Lu–C bonds was arbitrarily set to 3.1 Å. The hydrogen atoms on the methyl groups of the catalyst backbone have been omitted for the sake of clarity. Please note that the amino-/amidoallene moiety and the catalyst's backbone are displayed in a truncated fashion for several of the species.

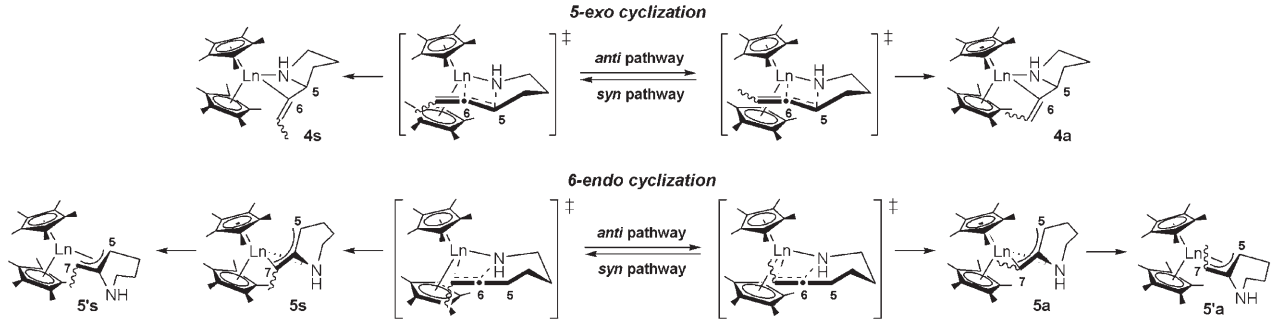

Scheme 2. Alternative pathways for 5-*exo* and 6-*endo* cyclization in the organolanthanide-mediated intramolecular hydroamination/cyclization of 1,3-disubstituted aminoallenes to afford functionalized five- and six-membered azacycles.

feasible ($\Delta G^{\ddagger} = 9.1$ kcal mol^{-1}), moderately exergonic ($\Delta G = -4.3$ kcal mol^{-1}) process that proceeds preferentially through the **3′**⇄**3s″**→**4s** *syn* pathway. A compact chair-like TS structure is encountered that is reflected in the estimated negative activation entropy of -11.0 cal mol^{-1} K^{-1}. The alternative **3′**⇄**3″**→**5**⇄**5′** path, which affords the six-membered azacycle, is significantly more expensive kinetically ($\Delta\Delta G^{\ddagger} > 9.7$ kcal mol^{-1}) for 1,3-disubstituted substrates owing to steric reasons.

To elaborate on the sensitivity of ring closure to steric demands further, the less encumbered monosubstituted 4,5-hexadien-1-ylamine substrate **1x** has also been studied (Table S1).[26a] In marked contrast to the 5-*exo* path, for which almost identical barriers for substrates **1** (*syn* pathway) and **1x** ($\Delta\Delta G^{\ddagger} = 0.1$ kcal mol^{-1}) are predicted, the relief of steric pressure reduces the 6-*endo* barrier substantially ($\Delta\Delta G^{\ddagger} = 10.4$ kcal mol^{-1}). Thus, for the monosubstituted substrate **1x** the 6-*endo* path becomes slightly favorable ($\Delta\Delta G^{\ddagger} = 0.6$ kcal mol^{-1}). This result is consistent with the observed product distribution for **1x**,[26b] and furthermore corroborates the marked influence of steric factors in controlling the regioselectivity of intramolecular C–N bond formation.

As a further crucial aspect, the possible supporting influence of additional substrate **1**, which is always present in excess under actual reaction conditions,[9d] has been probed computationally (see Figures S3 and S4 of the Supporting Information). Although the precursor exists predominantly as the **3′**-S adduct, additive substrate does not appear to fa-

cilitate 5-*exo* or 6-*endo* cyclization either kinetically or thermodynamically.

As revealed from Table 2, complexed **1** does not stabilize the TS structures and products in terms of enthalpy or free energy and therefore the substrate is unlikely to assist this process. Accordingly, the substrate must dissociate first from the precursor adduct prior to ring closure.

Protonolysis of azacyclic intermediates: Following the regioisomeric cyclization to generate **4** and **5**,**5**′, ensuing protonolysis by **1** leads to the respective cycloamine-amido–Lu compounds **6**–**8**, from which the cycloamine products **P6**–**P8** are liberated in a facile substitution by **1**. Regeneration of **3** initiates a new catalytic cycle (Scheme 1). The protonolysis of **4** and also of **5**,**5**′ by various pathways is explored in this section. The discussion is restricted to favorable pathways. A full characterization of structural (Figure S5–S10) and energetic (Table S2) aspects of all the investigated pathways is provided in the Supporting Information.

Starting with the protonolysis of the five-membered azacyclic intermediates, the initial formation of the precursor adduct **4**-S is uphill[22] at both the ΔH and ΔG surfaces (Table 3). The interaction of the azacycle **4** with lutetium through its nitrogen lone-pair becomes somewhat weakened upon complexation of **1**, but is nevertheless intact in **4**-S (Figure 2).[27] A TS structure that constitutes simultaneous N–H bond cleavage and C–H bond formation is encountered along the favorable path for proton transfer. Decay of the TS first leads to **6** from which the cycloamine products **P6** are liberated in a kinetically facile displacement[22] by incoming **1**. The C^8-methyl substituent does not incur significant unfavorable steric interactions with the Cp* methyl groups or the complexed substrate for proton transfer onto the tether's C^6 carbon of **4a** and **4s**, respectively (Figure 2). Hence, similar energy profiles are predicted in both cases (Table 3). Of the alternative **4s**+**1**→**6s** and **4a**+**1**→**6a** pathways, the first is kinetically favorable ($\Delta\Delta G^{\ddagger}=0.7$ kcal mol^{-1}), while the latter is driven by a slightly larger thermodynamic force ($\Delta\Delta G=2.2$ kcal mol^{-1}). Release of the pyrrolidines through **6s**/**6a**+**1**→**P6*Z***/**P6*E***+**3**′-S is an exergonic process ($\Delta G=-10.2/-9.8$ kcal mol^{-1}) that drives the overall protonolysis step strongly downhill.

Protonation following the kinetically favorable **4s**+**1**→**6s**(+**1**)→**P6*Z***(+**3**′-S) pathway is an exergonic process ($\Delta G=-11.9$ kcal mol^{-1}) with a barrier of 20.4 kcal mol^{-1} ($\Delta G^{\ddagger}$) that is associated with a negative activation entropy of -32.6 cal mol^{-1} K^{-1}. The large negative value for $\Delta S^{\ddagger}$ originates primarily from the first substrate association which affords the amine-amido–Lu adduct **4**-S.

Alternative routes starting from **5** and **5**′ have been explored for the protonolysis of the 6-*endo* cyclization intermediates (see Table S2 and Figure S5–S7 of the Supporting Information). Compound **5**′ appeared to be the direct precursor for the generation of cycloamines **P7** and **P8** through the regioisomeric **5**′+**1**→**7**(+**1**)→**P7**(+**3**′-S) and **5**′+**1**→**8**(+**1**)→**P8**(+**3**′-S) paths for proton transfer onto the C^7 and C^5 carbon atoms of the allylic functionality.[28] The initial substrate uptake[22] in **5**′ to yield adduct **5**′-S proceeds with a switch in the allylic–Lu coordination from an η^3-π to an η^1-σ mode.[29] Not surprisingly, the *anti*-allylic–Lu isomer **5a**′, which suffers from unfavorable repulsive interactions between the C^8-methyl group and the catalyst backbone (see the Intramolecular cyclization section), shows the greatest tendency for coordinative stabilization through substrate association (Table 3). Similar to the findings for five-membered azacyclic intermediates, protonolysis along the various pathways evolves through a σ-bond metathesis-type TS structure that represents simultaneous N–H bond cleavage and C–H bond formation in the proximity of the lutetium center. This TS structure does not appear to be particularly

Table 3. Enthalpies and free energies of activation and reaction for the protonolysis of the azacycle–Lu compounds **4** and **5** by aminoallene substrate **1** to afford the cycloamine-amido–Lu compounds **6**–**8** along various regioisomeric proton transfer paths.[a,b]

Cyclization path		Cycloamine-generating path	
	4-S/**5**′-S[c]	TS	Product[c]
5-*exo*			
syn pathway			2-[(*Z*)-prop-1-enyl]pyrrolidine
H-trf onto C-6 of **4s**	3.1/*12.6* (**4s**-S)[d]	10.7/*20.4* ($\Delta S^{\ddagger}=-32.6$ eu)[e]	−10.5/*−1.7* (**6s**)
anti pathway			2-[(*E*)-prop-1-enyl]pyrrolidine
H-trf onto C-6 of **4a**	6.5/*15.3* (**4a**-S)[d]	11.6/*21.1* ($\Delta S^{\ddagger}=-31.9$ eu)[e]	−12.7/*−3.9* (**6a**)
6-*endo*			
syn pathway			6-ethyltetrahydropyridine
H-trf onto C-7 of **5s**′	2.7/*11.2* (**5s**′-S)	5.9/*14.9* ($\Delta S^{\ddagger}=-33.3$ eu)[e]	−13.7/*−5.7* (**7**)
			2-[(*Z*)-ethylidene]piperidine
H-trf onto C-5 of **5s**′	−1.9/*6.5* (**5s**′-S)[d]	2.6/*11.7* ($\Delta S^{\ddagger}=-33.8$ eu)[e]	−11.4/*−3.2* (**8s**)
anti pathway			6-ethyltetrahydropyridine
H-trf onto C-7 of **5a**′	−3.3/*5.3* (**5a**′-S)	3.6/*13.4* ($\Delta S^{\ddagger}=-32.8$ eu)[e]	−20.4/*−12.2* (**7**)
			2-[(*E*)-ethylidene]piperidine
H-trf onto C-5 of **5a**′	−10.6/*−2.2* (**5a**′-S)[d]	3.2/*12.5* ($\Delta S^{\ddagger}=-31.3$ eu)[e]	−19.2/*−10.4* (**8a**)

[a] The total activation barriers, reaction energies, and activation entropies are given relative to {**4s**/**4a**+**1**} and {**5s**′/**5a**′+**1**} for the protonation of the 5-*exo* and 6-*endo* cyclization intermediates, respectively. [b] The enthalpies and free energies of activation ($\Delta H^{\ddagger}/\Delta G^{\ddagger}$) and reaction ($\Delta H/\Delta G$) are given in kilocalories per mole; the numbers in italic type are the Gibbs free-energies. [c] See the text (or Figure 2 and Figures S5–S7) for a description of the various isomers of the amine adducts **4**-S, **5**′-S, and of the cycloamine-amido–Lu product species **6**–**8**. [d] The precursor amine-adduct species is not identical to the related one reported in Table 2. [e] The activation entropy is given in entropic units ≡cal mol^{-1} K^{-1}.

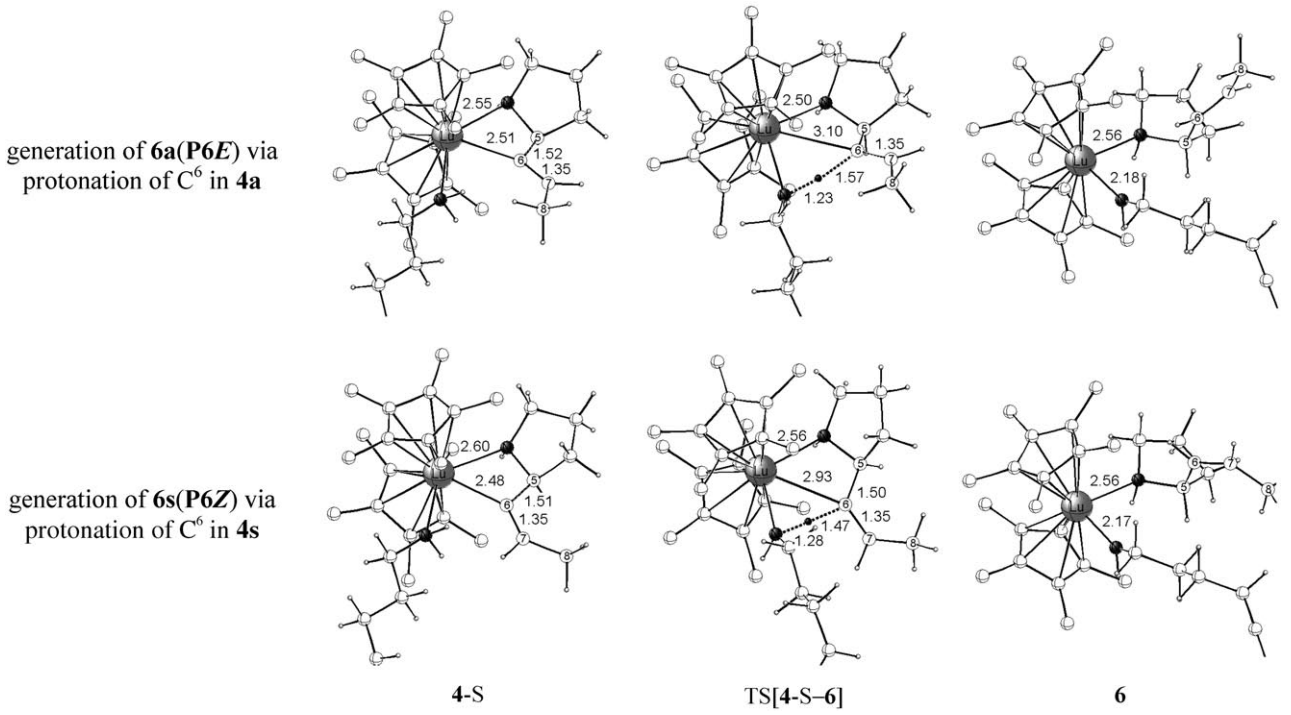

Figure 2. Selected structural parameters [Å] of the optimized structures of key species in the protonolysis of the azacycle–Lu intermediate **4** by aminoallene substrate **1** to afford the cycloamine-amido–Lu compounds **6a**, **6s** by alternative pathways. The cut-off for drawing Lu–C bonds was arbitrarily set to 3.1 Å. The hydrogen atoms on the methyl groups of the catalyst backbone have been omitted for the sake of clarity. Please note that the amino-/amidoallene moiety and the catalyst's backbone are displayed in a truncated fashion for several of the species.

sensitive to steric demands (see Figures S6 and S7) unlike the TS structure for 6-*endo* cyclization (see the Intramolecular cyclization section). As a result, the alternative pathways commencing from **5a′**/**5s′** have similar intrinsic barriers (i.e. relative to the direct **5a′**/**5s′** precursor species) for the paths that lead to **7**(**P7**) ($\Delta\Delta G^{\ddagger}_{int} = 1.5$ kcal mol^{-1}) and **8**(**P8**) ($\Delta\Delta G^{\ddagger}_{int} = 0.8$ kcal mol^{-1}). Thus, the terminal substrate C^8 substituent does not discriminate kinetically between the alternative *anti* and *syn* pathways, but it does discriminate thermodynamically between the two. As analyzed in the Intramolecular cyclization section, species **5a** (with **5a′** 8.4 kcal mol^{-1} higher in free energy) and **5s′** are the prevalent 6-*endo* cyclization products along the *anti* and *syn* pathways. The thermodynamic disfavor of precursor **5a′** renders the corresponding pathways to be more expensive energetically, when compared to the ones that start from **5s′**.

Of the competing **5s′**+**1**→**7**(+**1**)→**P7**(+**3′**-S) and **5s′**+**1**→**8s**(+**1**)→**P8Z**(+**3′**-S) paths, proton transfer onto the C^5 carbon atom is kinetically easier ($\Delta\Delta G^{\ddagger} = 3.2$ kcal mol^{-1}). Thus, **P8Z** would be the prevalent six-membered cycloamine that is initially formed in an overall exergonic process ($\Delta G = -19.1$ kcal mol^{-1}) provided that the generation of precursor **5′** (and **5**) is not precluded.

Excess substrate can be envisioned to support protonolysis in different ways. Additive substrate can, first, function as spectator ligands coordinated to the lanthanide, thereby acting primarily to counterbalance the reduction of the coordination sphere around lutetium, or secondly, participate directly as a mediator for proton transfer.[14a,30] Both alternatives have been explicitly probed in the protonation of **4** and **5′**. The examined paths are characterized structurally in Figures S8–S10 and energetically in Table S2. The additive substrate, either as spectator or as moderator, does not stabilize the TS for any of these paths on either the ΔH or the ΔG surface. Hence, the additive amine does not appear to facilitate these pathways kinetically. Accordingly, it must be concluded that excess substrate is unlikely to assist the protonolysis of azacycle–Lu intermediates **4** and **5′**(**5**). Although not explicitly examined, this conclusion can reasonably be extended to precatalyst activation (see the Precatalyst activation section).

Catalytic reaction course for the IHC of 1,3-disubstituted aminoallenes

Gibbs free-energy profile: The Gibbs free-energy profile for all the crucial elementary steps of the tentative catalytic cycle (Scheme 1) is presented in Scheme 3. The following conclusions can be drawn from Scheme 3 and the exploration of the crucial elementary steps reported in previous sections. 1) Intramolecular C=C insertion into the Lu–N functionality proceeds exclusively through 5-*exo* cyclization. The alternative 6-*endo* cyclization has a significantly higher barrier ($\Delta\Delta G^{\ddagger} = 9.7$ kcal mol^{-1}).[31] This barrier is predicted to be higher than that of the kinetically most difficult of the viable steps along the path that starts with 5-*exo* ring clo-

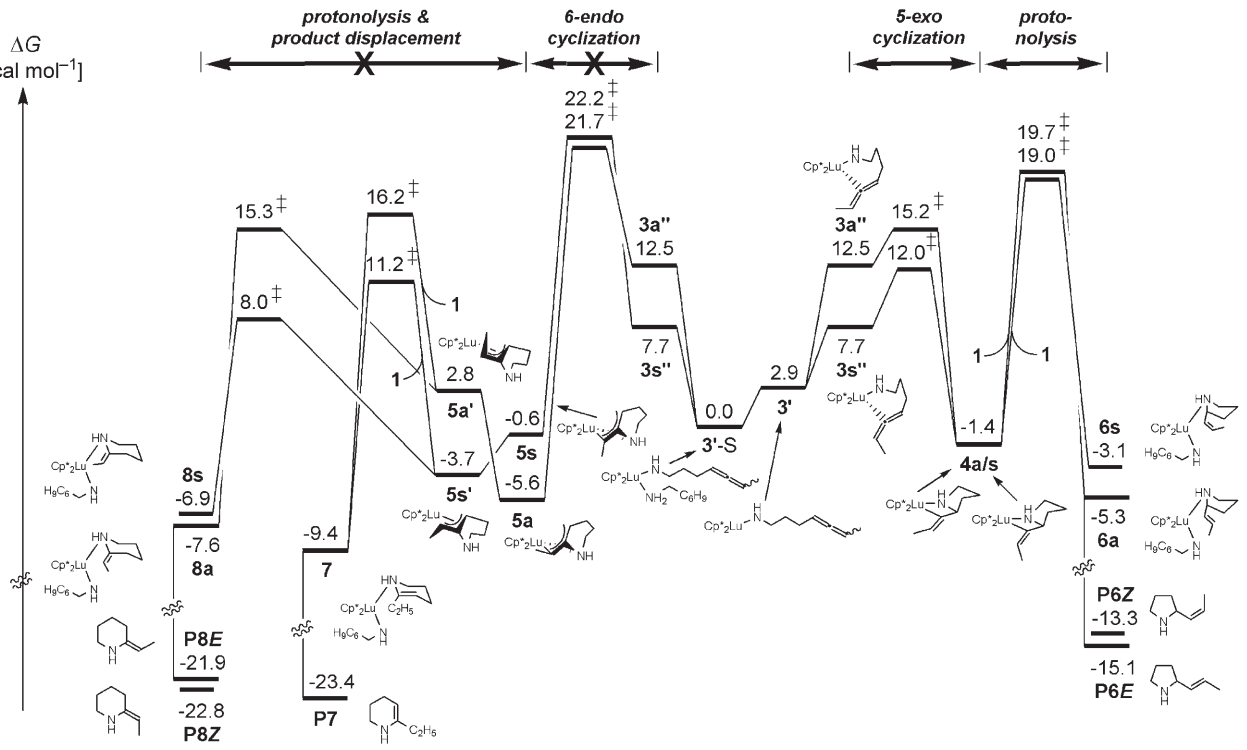

Scheme 3. Gibbs free-energy profile [kcal mol^{-1}] for the intramolecular hydroamination/cyclization of 4,5-heptadien-1-ylamine (**1**) mediated by the [Cp*$_2$LuCH(TMS)$_2$] precatalyst (**2**). The precursor species **4**-S/**5**′-S of the protonolysis step have been omitted for the sake of clarity. Cycloamine expulsion through **6**/**7**/**8**+**1**→**3**′-S+**P6**/**P7**/**P8** has been included.

sure. As a consequence, the complete sequence of steps that is initiated by 6-*endo* cyclization is not traversed in the catalytic process and is therefore of no relevance for further mechanistic considerations. 2) Compounds **3**′-S, **4**, and **6**, which is immediately converted back to **3**′-S through facile cycloamine product liberation, are predicted to be the thermodynamically prevalent species present in the catalytic reaction course. In accordance with the many experimental data,[3,5c,9] the amine-amidoallene–Lu adduct **3**′-S is the most likely candidate to be the catalyst's resting state under actual reaction conditions.[9d,32] 3) The substrate must first dissociate from **3**′-S prior to ring closure through 5-*exo* cyclization (see the Intramolecular cyclization section). 4) Protonolysis of **4** by **1** is also indicated to not be facilitated by additive substrate molecules. 5) Ring closure through the favorable **3**′-S→**3**′→**3s**″(+**1**)→**4s**(+**1**) 5-*exo* pathway is an essentially thermoneutral process ($\Delta G = -1.4$ kcal mol^{-1}) with a moderate intrinsic barrier ($\Delta G^{\ddagger}_{int} = 9.1$ kcal mol^{-1}, **3**′→**4s**) and is thus likely a facile and reversible process. 6) The **4**+**1**→**6**(+**1**)→**P6**(+**3**′-S) protonolysis has the highest kinetic barrier of all the viable steps. This turnover-limiting step is irreversible, driven by a large thermodynamic force.

These conclusions led us to suggest the mechanistic scenario shown in Scheme 4 for the organolanthanide-assisted IHC of 1,3-disubstituted aminoallenes. This scenario comprises of kinetically mobile substrate association and dissociation equilibria, K_1 and K_3, facile and reversible intramolecular C=C insertion into the Lu–N bond to yield azacyclic intermediates, and turnover-limiting protonation of the azacycle's tether functionality ($k_4 \equiv k_{prod}$). Starting from the resting state **3**′-S, the substrate first must become displaced prior to 5-*exo* cyclization to afford **3**′ with a nonchelating aminoallene functionality as the prevalent substrate-free amidoallene–Lu species. Ensuing facile **3**′→**4s** ring closure evolves through a compact chair-like TS structure with a negative activation entropy ($\Delta S^{\ddagger} = -11.0$ cal mol^{-1} K^{-1}). Cycloamine product formation proceeds first through rapid substrate association in **4s** and is followed by turnover-limiting proton transfer onto the azacycle's tether functionality. The entropic contributions for substrate association/dissociation equilibria K_1 ($\Delta S = 31.8$ cal mol^{-1} K^{-1}) and K_3 ($\Delta S = -31.7$ cal mol^{-1} K^{-1}) effectively compensate each other. Kinetic analysis assuming mobile equilibria K_1 and K_3 and applying steady-state concentrations[33a] for **4s**[33b] gives the rate law shown in Equation (2). This rate law is consistent with the empirical rate law [Eq. (1)] determined by experiment.

$$\text{velocity} = k_4 K_1 k_2 k_{-3} \times [\mathbf{3}'\text{-S}] \times [\mathbf{1}]^{-1} \qquad (2)$$

It predicts first-order behavior in [catalyst]. As a result of the associated equilibria K_1 and K_3, the kinetics is nevertheless zeroth-order in [substrate], although substrate **1** participates in the turnover-limiting step. For this mechanistic scenario, an effective total enthalpy barrier of 19.1 kcal mol^{-1} ($\Delta H^{\ddagger}_{tot}$)[32,34] is predicted for the most feasible protonolysis pathway for the generation of **6s** (**P6Z**), which is associated

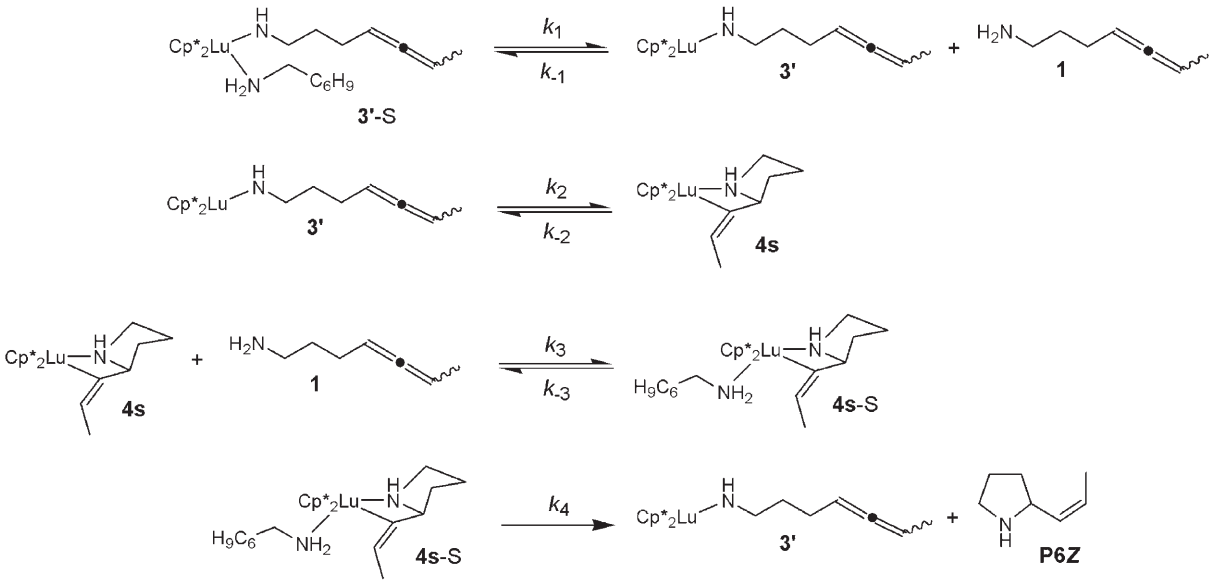

Scheme 4. Proposed mechanistic scenario for the organolanthanide-mediated intramolecular hydroamination/cyclization of 1,3-disubstituted aminoallenes, exemplified for the 4,5-heptadien-1-ylamine substrate.

with an estimated negative total activation entropy of $-8.2\ \mathrm{cal\,mol^{-1}\,K^{-1}}$ ($\Delta S^{\ddagger}_{\mathrm{tot}}$).[34] The computationally predicted kinetics agrees very well with measured data for the turnover-limiting step.[9d] The negative value of $\Delta S^{\ddagger}_{\mathrm{tot}}$ arises from the reaction entropy (ΔS) for cyclization and the intrinsic activation entropy ($\Delta S^{\ddagger}_{\mathrm{int}}$ for **4s**-S→**6s**) for protonation, while K_1/K_3 contributions compensate each other (see above). This yields an effective activation free-energy of $21.5\ \mathrm{kcal\,mol^{-1}}$ ($\Delta G^{\ddagger}_{\mathrm{tot}}$).[34] The proposed mechanistic scenario (Scheme 4), in combination with the computed free-energy profile (Scheme 3), is consistent with the empirical rate law [Eq. (1)] and accounts for crucial experimental observations.[9]The general mechanism proposed by Marks,[3] in which intramolecular cyclization is assumed to be rate-controlling (i.e. $k_2 \equiv k_{\mathrm{prod}}$) for various types of amine-tethered C–C unsaturated compounds, yields a rate law[35] that is consistent with the empirical law [Eq. (1)] and is similar to Equation (2). The following kinetics is predicted if **3′**→**4s** ring closure is turnover-limiting:[32,34] $\Delta H^{\ddagger}_{\mathrm{tot}} = 20.7\ \mathrm{kcal\,mol^{-1}}$ together with a large positive value for $\Delta S^{\ddagger}_{\mathrm{tot}}$ of 20.8 kcal $\mathrm{mol^{-1}\,K^{-1}}$ due to the K_1 equilibrium. This contrasts with experimental observations[9d] hence clearly revealing that the general mechanism by Marks is not operative in the cyclohydroamination of 1,3-disubstituted aminoallenes.

Factors governing regioselectivity and double-bond selectivity: Intramolecular C–N bond formation is the step that determines whether five- or six-membered azacycles are formed. Of the two regioisomeric paths for ring closure, both of which are equally feasible in terms of electronic factors,[36] the 5-*exo* path is predicted to be distinctly less expensive kinetically ($\Delta\Delta G^{\ddagger} > 9.7\ \mathrm{kcal\,mol^{-1}}$) than the 6-*endo* cyclization of 1,3-disubstituted aminoallenes for steric reasons. The computed sufficiently large kinetic gap clearly reveals the ring closure to take place with almost complete regioselectivity, to yield the five-membered azacycle exclusively. This rationalizes why tetrahydropyridines are not among the reaction products. Steric effects are furthermore seen to discriminate between alternative pathways for the favorable 5-*exo* cyclization process. This, however, is of little relevance for the cycloamine **P6*Z***/**P6*E*** product ratio as the barriers for **3′**⇄**3a″**→**4a** and **3′**⇄**3s″**→**4s** are lower than that for rate-determining protonolysis. Hence, the energetically equivalent azacyclic intermediates **4a** and **4s** are populated to the same extent. As a consequence, the distribution of the pyrrolidine products **P6*Z*** and **P6*E*** is entirely kinetically regulated.

Of the alternative **4a**+**1**→**6a**(+**1**)→**P6*E***(+**3′**-S) and **4s**+**1**→**6s**(+**1**)→**P6*Z***(+**3′**-S) pathways, **4s** exhibits a larger aptitude for protonation of its C^6 carbon tether. The predicted kinetic gap of $0.7\ \mathrm{kcal\,mol^{-1}}$ ($\Delta\Delta G^{\ddagger}$) reveals that 2-[(*Z*)-prop-1-enyl)pyrrolidine **P6*Z*** is the cycloamine that is predominantly formed. It is also in remarkably good agreement with the observed **P6*Z***/**P6*E*** product ratio[9d,37] and rationalizes the observed good *Z* double-bond selectivity.[9d]

Organolanthanide-mediated IHC of 1,3-disubstituted aminoallenes and conjugated aminodienes: A mechanistic comparison: Similar mechanistic scenarios have been proposed computationally for conjugated aminodienes[14a] and 1,3-disubstituted aminoallenes that differ from the general proposal by Marks.[3] They entail kinetically rapid substrate association and dissociation equilibria, facile and reversible intramolecular C–C insertion into the Ln–N bond, and the turnover-limiting protonation of the azacycle's tether functionality. Despite the apparent similarity of the mechanisms

operative for the two substrate classes, the cyclization and protonolysis steps nevertheless exhibit unique characteristics.

A distinct kinetic preference for C–N bond formation through the exocyclic pathway is predicted for both substrate classes such that ring closure proceeds with almost complete regioselectivity. This is primarily due to electronic factors for aminodienes,[14a,36] while steric effects are crucial in the reaction of 1,3-disubstituted aminoallenes (see the Intramolecular cyclization section). Commencing with substrate-free precursor species with a nonchelating η^1-amido–Ln functionality, ring closure evolves through chair-like TS structures. The estimated value of $\Delta S^{\neq}$ [-11.0 and -12.5 cal mol^{-1} K^{-1} for 4,5-heptadien-1-ylamine and (4*E*,6)-heptadien-1-amine,[14a] respectively] indicates the TS structure to be slightly less compact for aminoallenes than for aminodienes. Intramolecular C–N bond formation for the less activated allenic C=C linkage has a higher free-energy barrier (9.1 kcal mol^{-1}) than the diene functionality (7.7 kcal mol^{-1}).[14a,21]

For both substrate classes, a σ-bond metathesis-type TS structure is encountered along the favorable path for the protonolysis of the azacycle's side chain. Commencing with the corresponding azacyclic precursor and subsequent substrate complexation, proton transfer onto the terminal carbon atom of the allylic functionality is less expensive kinetically ($\Delta G^{\neq} = 16.0$ kcal mol^{-1})[14a] than the protonation of the tether's internal carbon for 1,3-disubstituted aminoallene substrates ($\Delta G^{\neq} = 20.4$ kcal mol^{-1}). Note that the thermodynamic gap between the protonolysis precursor and the amine-amido–Ln catalyst's resting state also influences the effective kinetics ($\Delta G^{\neq}_{tot}$) of the turnover-limiting protonolysis.

The computationally predicted effective total free-energy barriers ($\Delta G^{\neq}_{tot}$) for protonolysis in the IHC of 4,5-heptadien-1-ylamine (21.5 kcal mol^{-1}) and (4*E*,6)-heptadien-1-amine (18.2 kcal mol^{-1})[14a] are in remarkably good agreement with the measured turnover-limiting barriers[38] and reflect the higher turnover numbers observed for conjugated aminodienes.[3]

Conclusions

A comprehensive computational investigation is presented herein that elucidates the detailed mechanism for the organolanthanide-mediated intramolecular hydroamination/cyclization (IHC) of 1,3-disubstituted aminoallenes. This study has been conducted for a prototypical achiral lutetiocene-based [(η^5-Me_5C_5)$_2$LuCH(SiMe$_3$)$_2$] precatalyst and 4,5-heptadien-1-ylamine substrate, for which a detailed kinetic investigation has been reported.[9a,c] Alternative pathways have been scrutinized for each of the crucial elementary steps of a tentative catalytic cycle (Scheme 1) by means of a reliable DFT method. The presented computational study provides, for the first time, a detailed insight into the salient features of the reaction in terms of structural and energetic aspects. The following objectives have been accomplished. 1) A mechanistic scenario (Scheme 4) has been proposed that a) reveals the identity of the turnover-limiting step, b) is consistent with the empirical rate law determined by experiment, and c) accounts for crucial experimental observations. This mechanism entails kinetically rapid substrate association and dissociation equilibria, facile and reversible intramolecular allenic C=C insertion into the Ln–N bond, and turnover-limiting protonation of the azacycle's tether functionality with the amine-amidoallene–Ln adduct **3′**-S being the catalyst's resting state. The computed effective kinetics ($\Delta G^{\neq}_{tot} = 21.5$ kcal mol^{-1}) is in good agreement with the experimental data. 2) This mechanistic scenario bears resemblance to the mechanism that has been proposed in a recent computational exploration of the cyclohydroamination of conjugated aminodienes.[14a] It revises the general mechanism for organolanthanide-assisted IHC proposed by Marks[3] for both 1,3-disubstituted aminoallene and conjugated aminodiene substrates. The unique features of the IHC of the two substrate classes have been discussed. 3) The thermodynamic and kinetic factors that control the regio- and stereoselectivity of cycloamine production have been elucidated.

This study has provided a deeper insight into the catalytic structure–reactivity relationships in organolanthanide-assisted cyclohydroamination of unsaturated C–C functionalities. The achievements reported herein are a crucial prerequisite for 1) the rational design of new improved catalysts and 2) elucidating the factors that are effective in controlling the diastereoselectivity of aminoallene IHC. These aspects will be addressed in forthcoming investigations.

Acknowledgements

I thank Professor Tom Ziegler (University of Calgary, Canada) for his generous support. Excellent service by the computer centers URZ Halle and URZ Magdeburg is gratefully acknowledged.

[1] a) L. S. Hegedus, *Angew. Chem.* **1988**, *100*, 1147; *Angew. Chem. Int. Ed. Engl.* **1988**, *27*, 1113; b) D. M. Roundhill, *Catal. Today* **1997**, *37*, 155; c) T. E. Müller, M. Beller, *Chem. Rev.* **1998**, *98*, 675; d) G. A. Molander, *Chemtracts: Org. Chem.* **1998**, *11*, 237; e) J. J. Brunet, D. Neibecker in *Catalytic Heterofunctionalization* (Eds.: A. Togni, H. Grützmacher), Wiley-VCH, Weinheim, **2001**, pp. 91–141; f) M. Nobis, B. Drießen-Hölscher, *Angew. Chem.* **2001**, *113*, 4105; *Angew. Chem. Int. Ed.* **2001**, *40*, 3983; g) R. Taube in *Applied Homogeneous Catalysis with Organometallic Complexes* (Eds.: B. Cornils, W. A. Herrmann), Wiley-VCH, Weinheim, Germany, **2002**, pp. 513–524; h) F. Pohlki, S. Doye, *Chem. Soc. Rev.* **2003**, *32*, 104; i) P. W. Roesky, T. E. Müller, *Angew. Chem.* **2003**, *115*, 2812; *Angew. Chem. Int. Ed.* **2003**, *42*, 2708; j) K. C. Hultzsch, *Adv. Synth. Catal.* **2005**, *347*, 367.

[2] a) T. J. Marks, R. D. Ernst in *Comprehensive Organometallic Chemistry* (Eds.: G. Wilkinson, F. G. A. Stone, E. W. Abel), Pergamon Press, Oxford, **1982**, Chapter 21; b) W. J. Evans, *Adv. Organomet. Chem.* **1985**, *24*, 131; c) C. J. Schaverien, *Adv. Organomet. Chem.* **1994**, *36*, 283; d) H. Schumann, J. A. Meese-Marktscheffel, L. Esser, *Chem. Rev.* **1995**, *95*, 865; e) F. T. Edelmann in *Comprehensive Organometallic Chemistry* (Eds.: G. Wilkinson, F. G. A. Stone, E. W. Abel), Pergamon Press, Oxford, **1995**, Vol. *4*, Chapter 2; f) R.

Anwander, W. A. Herrmann, *Top. Curr. Chem.* **1996**, *179*, 1; g) F. T. Edelmann, *Curr. Chem.* **1996**, *179*, 247; h) *Topics in Organometallic Chemistry* (Ed.: S. Kobayashi), Springer, Berlin, **1999**; i) M. N. Bochkarev, *Chem. Rev.* **2002**, *102*, 2089; j) S. Arndt, J. Okuda, *Chem. Rev.* **2002**, *102*, 1953; k) F. T. Edelmann, D. M. M. Freckmann, H. Schumann, *Chem. Rev.* **2002**, *102*, 1851; l) H. C. Aspinall, *Chem. Rev.* **2002**, *102*, 1807.

[3] S. Hong, T. J. Marks, *Acc. Chem. Res.* **2004**, *37*, 673.

[4] G. A. Molander, J. A. C. Romero, *Chem. Rev.* **2002**, *102*, 2161.

[5] a) M. R. Gagné, T. J. Marks, *J. Am. Chem. Soc.* **1989**, *111*, 4108; b) M. R. Gagné, S. P. Nolan, T. J. Marks, *Organometallics* **1990**, *9*, 1716; c) M. R. Gagné, T. J. Marks, *J. Am. Chem. Soc.* **1992**, *114*, 275; d) M. A. Giardello, V. P. Conticello, L. Brard, M. R. Gagné, T. J. Marks, *J. Am. Chem. Soc.* **1994**, *116*, 10241.

[6] a) G. A. Molander, E. D. Dowdy, *J. Org. Chem.* **1998**, *63*, 8983; b) A. T. Gilbert, B. L. Davis, T. J. Emge, R. D. Broene, *Organometallics* **1999**, *18*, 2125; c) G. A. Molander, E. D. Dowdy, *J. Org. Chem.* **1999**, *64*, 6515; d) Y. K. Kim, T. Livinghouse, J. E. Bercaw, *Tetrahedron Lett.* **2001**, *42*, 2944; e) G. A. Molander, E. D. Dowdy, S. K. Pack, *J. Org. Chem.* **2001**, *66*, 4344; f) Y. K. Kim, T. Livinghouse, *Angew. Chem.* **2002**, *114*, 3797; *Angew. Chem. Int. Ed.* **2002**, *41*, 3645; g) P. N. O'Shaughnessy, P. D. Knight, C. Morton, K. M. Gillespie, P. Scott, *Chem. Commun.* **2003**, 1770.

[7] a) Y. Li, P.-F. Fu, T. J. Marks, *Organometallics* **1994**, *13*, 439; b) Y. Li, T. J. Marks, *J. Am. Chem. Soc.* **1996**, *118*, 707; c) Y. Li, T. J. Marks, *J. Am. Chem. Soc.* **1996**, *118*, 9295; d) Y. Li, T. J. Marks, *J. Am. Chem. Soc.* **1998**, *120*, 1757.

[8] a) M. R. Bürgstein, H. Berberich, P. W. Roesky, *Organometallics* **1998**, *17*, 1452; b) M. R. Bürgstein, H. Berberich, P. W. Roesky, *Chem. Eur. J.* **2001**, *7*, 7078; c) D. V. Gribkov, K. C. Hultzsch, F. Hampel, *Chem. Eur. J.* **2003**, *9*, 4796; d) A. Zulys, T. K. Panda, M. T. Gamer, P. W. Roesky, *Chem. Commun.* **2004**, 2584.

[9] a) V. M. Arredondo, F. E. McDonald, T. J. Marks, *J. Am. Chem. Soc.* **1998**, *120*, 4871; b) V. M. Arredondo, S. Tian, F. E. McDonald, T. J. Marks, *J. Am. Chem. Soc.* **1999**, *121*, 3633; c) V. M. Arredondo, F. E. McDonald, T. J. Marks, *Organometallics* **1999**, *18*, 1949; d) typical reaction conditions for the organolanthanide-mediated cycloamination of aminoallenes are: 40–70-fold molar excess of the substrate [for example, 4,5-heptadien-1-ylamine (**1**)] together with the precatalyst {for example, $[Cp^*_2LuCH(SiMe_3)_2]$ (**2**)} at 25 °C in noncoordinating solvents, such as benzene, toluene, pentane, and cyclohexane; the following kinetics were experimentally determined for the cycloamination of 4,5-heptadien-1-ylamine (**1**) mediated by the $[Cp^*_2LuCH(SiMe_3)_2]$ precatalyst (**2**), which affords an 88:12 mixture of *Z*/*E* isomers **P6*Z*** and **P6*E*** of 2-(prop-1-enyl)pyrrolidine exclusively: $\Delta H^{\neq} = 16.9(1.3)$ kcal mol^{-1} and $\Delta S^{\neq} = -16.48(4.3)$ kcal mol^{-1} K^{-1} (see also ref. [9c]).

[10] a) S. Hong, T. J. Marks, *J. Am. Chem. Soc.* **2002**, *124*, 7886; b) S. Hong, A. M. Kawaoka, T. J. Marks, *J. Am. Chem. Soc.* **2003**, *125*, 15878; c) S. Hong, S. Tian, M. V. Metz, T. J. Marks, *J. Am. Chem. Soc.* **2003**, *125*, 14768.

[11] a) L. Ackermann, R. G. Berman, *Org. Lett.* **2002**, *4*, 1475; b) L. Ackermann, R. G. Bergman, R. N. Loy, *J. Am. Chem. Soc.* **2003**, *125*, 11956; c) J. M. Hoover, J. R. Petersen, J. H. Pikul, A. R. Johnson, *Organometallics* **2004**, *23*, 4614.

[12] a) S. Arseniyadis, J. Gore, *Tetrahedron Lett.* **1983**, *24*, 3997; b) R. Kinsman, D. Lathbury, P. Vernon, T. Gallagher, *J. Chem. Soc., Chem. Commun.* **1987**, 243; c) D. N. A. Fox, T. Gallagher, *Tetrahedron* **1990**, *46*, 4697; d) M. Al-Masum, M. Meguro, Y. Yamamoto, *Tetrahedron Lett.* **1997**, *38*, 6071; e) M. Meguro, Y. Yamamoto, *Tetrahedron Lett.* **1998**, *39*, 5421.

[13] A. Motta, G. Lanza, I. L. Fragala, T. J. Marks, *Organometallics* **2004**, *23*, 4097.

[14] a) S. Tobisch, *J. Am. Chem. Soc.* **2005**, *127*, 11979; b) for a computational mechanistic study of the organolanthanide-mediated intermolecular hydroamination of 1,3-dienes and primary amines, see: S. Tobisch, *Chem. Eur. J.* **2005**, *11*, 6372.

[15] There is substantial precedent for η^3-allylic structures in organo-f-element chemistry, for example, see: a) G. Jeske, H. Lauke, H. Mauermann, P. N. Swepston, H. Schumann, T. J. Marks, *J. Am. Chem. Soc.* **1985**, *107*, 8091; b) E. Bunel, B. J. Burger, J. E. Bercaw, *J. Am. Chem. Soc.* **1988**, *110*, 976; c) S. P. Nolan, D. Stern, T. J. Marks, *J. Am. Chem. Soc.* **1989**, *111*, 7844; d) W. J. Evans, T. A. Ulibarri, J. W. Ziller, *J. Am. Chem. Soc.* **1990**, *112*, 2314; e) A. Scholz, A. Smola, J. Scholz, J. Löbel, H. Schimann, K.-H. Thiele, *Angew. Chem.* **1991**, *103*, 444; *Angew. Chem. Int. Ed. Engl.* **1991**, *30*, 435; f) W. J. Evans, R. A. Keyer, G. W. Rabe, D. K. Drummond, J. W. Ziller, *Organometallics* **1993**, *12*, 4664; g) W. J. Evans, S. L. Gonzales, J. W. Ziller, *J. Am. Chem. Soc.* **1994**, *116*, 2600.

[16] a) R. Ahlrichs, M. Bär, M. Häser, H. Horn, C. Kölmel, *Chem. Phys. Lett.* **1989**, *162*, 165; b) O. Treutler, R. Ahlrichs, *J. Chem. Phys.* **1995**, *102*, 346; c) K. Eichkorn, O. Treutler, H. Öhm, M. Häser, R. Ahlrichs, *Chem. Phys. Lett.* **1995**, *242*, 652.

[17] a) P. A. M. Dirac, *Proc. Cambridge Philos. Soc.* **1930**, *26*, 376; b) J. C. Slater, *Phys. Rev.* **1951**, *81*, 385; c) S. H. Vosko, L. Wilk, M. Nussiar, *Can. J. Phys.* **1980**, *58*, 1200; d) A. D. Becke, *Phys. Rev. A* **1988**, *38*, 3098; e) J. P. Perdew, *Phys. Rev. B* **1986**, *33*, 8822; *Phys. Rev. B* **1986**, *34*, 7406.

[18] For example, see: a) S. Tobisch, Th. Nowak, H. Boegel, H. *J. Organomet. Chem.* **2001**, *619*, 24; b) H. Heiber, O. Gropen, J. K. Laerdahl, O. Swang, U. Wahlgreen, *Theor. Chem. Acc.* **2003**, *110*, 118.

[19] S. Tobisch, *Chem. Eur. J.* **2005**, *11*, 3113.

[20] For further details, see: www.struked.de.

[21] a) Computational studies of the IHC of prototypical 1,3-disubstituted aminoallene and conjugated aminodiene substrates (see ref. [14a]) have been conducted for $[Cp^*_2LnCH(TMS)_2]$ precatalysts of identical type but with different active lanthanide centers (Ln = La and Lu for aminodiene and aminoallene substrates, respectively). The Ln^{3+} ion size and skeletal substrate substitutions, however, have been reported to have a significant influence on the turnover-limiting barrier (see refs. [9c,21b]) which can likely be supposed for other steps as well. Accordingly, the computationally predicted energy profiles for the IHC of 4,5-heptadien-1-ylamine and (4*E*,6)-heptadien-1-amine cannot be compared directly in a strict sense. Turnover frequencies of the same magnitude have been measured for the IHC of 1,3-disubstituted aminoallene catalyzed by Lu- and La-based systems, such that a semiquantitative comparison of the energetics for the two substrates seems to be suitable. b) For metal and ancillary ligand effects on aminodiene cyclohydroamination reactions, see: S. Hong, A. M. Kawaoka, T. J. Marks, *J. Am. Chem. Soc.* **2003**, *125*, 15878.

[22] Examination by a linear-transit approach gave no indication that this process is associated with a significant enthalpic barrier.

[23] R. D. Shannon, *Acta Crystallogr., Sect. A* **1976**, *A32*, 751.

[24] For NMR evidence of rapid amido/amine permutation and association/dissociation of amine substrates, see ref. [5c].

[25] The located adduct species **3″**-S is characterized by only a weak amidoallene–Ln chelating interaction (cf. Figure S3).

[26] a) The extension of our study to the 4,5-hexadien-1-ylamine substrate **1x**, which differs from **1** by the replacement of the C^8-methyl substituent by a hydrogen atom, is restricted to the intramolecular cyclization step. The complete catalytic cycle for the IHC of **1x** in the presence of precatalyst **2** will be reported elsewhere. b) Under identical reaction conditions, as for substrate **1** (see ref. [9c]), a 10:90 ratio of 5-*exo*-(2-vinylpyrrolidine)/6-*endo*-(2-methyltetrahydropyridine) products is observed for the IHC of **1x** in the presence of **2** (see ref. [9a,c]).

[27] Substrate adducts **4**-S with a disrupted azacycle–Lu interaction are energetically unfavorable. For more details see the Supporting Information.

[28] The alternative path to **P7** through **5**+**1**→**7**(+**1**)→**P7**(+**3′**-S) proton transfer onto the C^7 carbon of **5** is predicted to be kinetically less likely than the path commencing from **5′** (see Table S2 and Figure S5 of the Supporting Information).

[29] The **5s′**+**1**→**7**(+**1**)→**P7**(+**3′**-S) pathway is an exception in which the η^3-allylic–Lu interaction in **5s′**-S remains essentially intact (see Figure S6 of the Supporting Information).

[30] H. M. Senn, P. E. Blöchl, A. Togni, *J. Am. Chem. Soc.* **2000**, *122*, 4098.

[31] In the comparison of the energetics of the alternative regioisomeric pathways, the respective favorable stereochemical pathways were considered.

[32] Please note that the condensed free-energy profile is computed for standard conditions (298.15 K, 1 atm, stoichiometric amount of aminoallene substrate). The large excess of substrate **1**, however, favors the generation of adducts like **3′**-S. The correction for **3′**$+$**1**$\rightarrow$**3′**-S adduct formation for concentration effects according to $\Delta G = \Delta G^{\circ} - RT \times \ln([\mathbf{3'}\text{-S}] \times [\mathbf{3'}]^{-1} \times [\mathbf{1}]^{-1})$ reduces the free energy (and the enthalpy) by $RT \times \ln([\mathbf{1}]^{-1})$, which amounts to 2.5 kcal mol^{-1} on consideration of real reaction conditions (70 molar excess of **1**, 298.15 K, 1 atm (see ref. [9d]).

[33] a) J. H. Espenson, *Chemical Kinetics and Reaction Mechanisms*, 2nd ed., McGraw-Hill, New York, **1995**. b) Intermediates **4a** and **4s** are likely to be transient species and are thus present in negligible stationary concentrations because their formation through reversible **3′**$\rightarrow$**4a**/**4s** 5-*exo* cyclization and ensuing **4a**/**4s**$+$**1**$\rightarrow$**4a**-S/**4s**-S substrate association are facile processes.

[34] The total enthalpies (ΔH_{tot}), free energies (ΔG_{tot}), and entropies (ΔS_{tot}) are given relative to the catalyst's resting state **3′**-S, and are corrected by the respective number of substrate molecules.

[35] Under similar assumptions to those made for Equation (2), one obtains: velocity $= k_2 K_1 \times [\mathbf{3'}\text{-S}] \times [\mathbf{1}]^{-1}$.

[36] The reader is referred to Baldwin's rules for ring closure which predict both exo- and endocyclic paths to be favorable for aminoallenes, while for aminodienes only the exocyclic path is predicted to be favorable. See: J. March, *Advanced Organic Chemistry*, 4th ed., Wiley, New York, **1992**, pp. 212–214.

[37] The kinetic gap of 0.7 kcal mol^{-1} ($\Delta\Delta G^{\neq}$) corresponds to a **P6*Z***/**P6*E*** ratio of 76.5:23.5 (298.15 K) on application of Maxwell–Boltzmann statistics. The experimentally observed 88:12 ratio for **P6*Z***/**P6*E*** transforms into $\Delta\Delta G^{\neq} = 1.18$ kcal mol^{-1} (298.15 K).

[38] The following effective kinetics have been measured for IHC in the presence of [Cp*$_2$LnCH(TMS)$_2$] precatalysts: 1,3-disubstituted aminoallenes (4,5-heptadien-1-ylamine), $\Delta G^{\neq}_{tot} = 19.2$–$24.4$ kcal mol^{-1} (see ref. [9d]); conjugated aminodienes [(4*E*,6)-heptadien-1-amine], $\Delta G^{\neq}_{tot} = 19.4$–$20.9$ kcal mol^{-1} (see ref. [21b]).

Received: August 21, 2005
Published online: December 9, 2005

